

# Model-independent Test of the Cosmic Anisotropy with Inverse Distance Ladder

Zong-Fan Yang<sup>1</sup>, Da-Wei Yao<sup>2</sup>, and Ke Wang<sup>1,3,4,5\*</sup>

<sup>1</sup>*School of Physical Science and Technology, Lanzhou University, Lanzhou 730000, China*

<sup>2</sup>*Beijing Zhihuo Technology Co., Ltd, Beijing 100000, China*

<sup>3</sup>*Institute of Theoretical Physics & Research Center of Gravitation, Lanzhou University, Lanzhou 730000, China*

<sup>4</sup>*Key Laboratory of Quantum Theory and Applications of MoE, Lanzhou University, Lanzhou 730000, China and*

<sup>5</sup>*Lanzhou Center for Theoretical Physics & Key Laboratory of Theoretical Physics of Gansu Province, Lanzhou University, Lanzhou 730000, China*

(Dated: July 30, 2024)

The Universe with the cosmic anisotropy will have a preferred direction of expansion. Therefore, reconstructing the expansion history by Gaussian Process (GP) can be used to probe the cosmic anisotropy model-independently. In this paper, for the luminosity distance  $d_L(z)$  reconstruction, we turn to the inverse distance ladder where the type Ia supernova (SNIa) from the Pantheon+ sample determine the relative distances and the strongly gravitationally lensed quasars from H0LiCOW sample anchor these relative distances with some absolute distance measurements. By isolating the anisotropic information maybe carried by the Hubble constant  $H_0$  and obtaining the constraint on the intrinsic parameter of SNIa, the absolute magnitude  $M = -19.2522^{+0.0270}_{-0.0279}$  (at 68% CL), we find that  $d_L(z)$  reconstructions from samples located in different region of the Galactic coordinate system are almost consistent with each other and only a very weak preference for the cosmic anisotropy is found.

## I. INTRODUCTION

The cosmological principle hypothesizes that the Universe features homogeneity and isotropy on large scales. Ground on some basic important assumptions, including the cosmological principle, the standard model of particle physics and Einstein's theory of gravity, the standard model of cosmology is established. More precisely, according to the latest cosmic microwave background (CMB) observations [1], the measurements of galaxy clustering and weak gravitational lensing [2] and the measurements of baryon acoustic oscillation (BAO) [3–5], the Lambda cold dark matter ( $\Lambda$ CDM) model is supported. Despite its successes on large cosmic scales, there are some underlying crises appearing on small scales, such as a dipole with larger amplitude in the quasar sky [6], a smaller amplitude of matter fluctuations  $\sigma_8$  obtained from cluster counts [7] and a larger local value of the Hubble constant  $H_0$  [8]. Besides general relativity (GR), dark energy model or treatments of systematic uncertainty, these tensions also challenge the cosmological principle. Therefore, it is imperative to know to what extent the cosmological principle is the truth, hence the need for a further test of the local cosmic inhomogeneity and anisotropy on small scales.

The most simple methods to test the cosmic anisotropy are based on the type Ia supernovae (SNIa) data, such as the Pantheon+ sample [9]. Since a large number of SNIa spread out in the Galactic coordinate system, one straightforward method is to divide the whole SNIa sample into several subsets according to its distribution.

In particular, the hemisphere comparison method divides the whole sample into two data subsets and investigates the discrepancy between these two opposite hemispheres [10, 11]. To further probe the fine structure that might be smoothed out, one can use HEALPix [12] to divide the whole SNIa sample into several data subsets at a time. Another common method is the dipole fitting method, which assumes the observation of every SNIa depends on a cosmic priori dipole [13]. However, these methods are model-dependent. More precisely, in these methods, the luminosity distance  $d_L$  is calculated in a specific cosmological model, such as in the  $\Lambda$ CDM model [14–18],  $w$ CDM model [19], CPL model [20], Finsterli model [21], ALTB model [22] and so on.

If  $d_L$  can be calculated model-independently, one can make a model-independent test of the cosmic anisotropy with SNIa data. In fact, there are several ways to realize this ambition. For example, there are a family of polynomials in the indeterminate of redshift variables approximating  $d_L$  model-independently [23–25]. Similarly,  $d_L$  can be expressed model-independently by the cosmographic parameters according to the well-known cosmographic approach [26, 27]. As for the completely data-driven nonparametric approach,  $d_L$  can be reconstructed model-independently by the artificial neural network (ANN) [28]. In some cases, one may only care about the relative distances from SNIa, where one can turn to Gaussian Process (GP) to reconstruct the dimensionless luminosity distance  $D_L \equiv d_L H_0 / c$  [29, 30]. In this paper, we will use GP to perform the reconstruction of  $D_L$  from the Pantheon+ sample [9].

Given the relative distances from SNIa, one should anchor them with an absolute distance measurement. For the local distance ladder,  $H_0$  and the absolute magnitude  $M$  of SNIa are usually calibrated by very local Cepheids [8, 9]. Although these very local absolute dis-

---

\*Corresponding author: wangkey@lzu.edu.cn

tance measurements are almost completely insensitive to the cosmological background model, they are too local to consider their distribution, hence no anisotropic information from them. On the contrary, the inverse distance ladder can be calibrated at high redshift using other independent measurements, such as the sound horizon at radiation drag  $r_d$  determined by CMB observations [31, 32], the time delays  $\Delta t_{j,1}$  between Supernova Refsdal's  $j$ th and first appearances [33, 34], the time-delay distance  $d_{\Delta t}$  of strongly gravitationally lensed quasars [25, 35–39] and so on. If anchors at high redshift also spread out in the Galactic coordinate system, they may carry certain anisotropic information, just as SNIa sample does. Therefore, in this paper, we will use  $d_{\Delta t}$  measurements of six lensed quasars from the H0LiCOW sample [35] to anchor  $D_L$  reconstructions from the Pantheon+ sample [9]. That is to say, we can model-independently test the cosmic relative or absolute anisotropy with  $D_L$  reconstructions only or the combination of  $D_L$  reconstructions and  $d_{\Delta t}$  measurements respectively.

This paper is organized as follows. In section II, we introduce a model-independent method and the widespread data through the Galactic coordinate system for  $D_L(z)$  reconstruction, namely GP and the Pantheon+ sample [9]. Meanwhile, we present the anchors from the H0LiCOW sample [35] for the inverse distance ladder. In section III, we show the reconstruction of  $d_L(z)$  from different dataset which serves as the probe of the cosmic anisotropy in our paper. Finally, a brief summary and discussions are included in section IV.

## II. METHODOLOGY AND DATA

In this section, we provide a brief summary of the model-independent GP algorithm, the SNIa data used for the Universe expansion history reconstruction and the strong gravitational lenses data used to anchor the inverse distance ladder.

### A. Gaussian Process

While the Gaussian distribution describes the distribution of a random variable with mean and variance, GP describes the distribution of a function  $f(x)$  with mean  $\mu(x)$ , variance  $\sigma^2(x)$  and kernel  $k(x, x')$ . There are several choices of kernel function, such as the squared exponential kernel, Matern (5/2) kernel, Matern (7/2) kernel and Matern (9/2) kernel. Here we only use the squared exponential kernel

$$k(x, x') = \sigma_f^2 \exp \left[ -\frac{(x - x')^2}{2l^2} \right], \quad (1)$$

where  $\sigma_f$  and  $l$  are the GP hyperparameters. The former one determines the correlation strength between  $f(x)$  and  $f(x')$ , the latter one is the correlation length determining which  $f(x')$  should be correlated with  $f(x)$ .

Before  $f(x)$  is reconstructed, these two hyperparameters should be known. Given the observed data  $\{\mathbf{x}, \mathbf{y} = f(\mathbf{x}) \pm \sigma(\mathbf{x})\}$ ,  $\sigma_f$  and  $l$  can be trained by maximizing the marginal likelihood [30, 40]

$$\begin{aligned} \ln \mathcal{L} &= \ln P(\mathbf{y}|\mathbf{x}, \sigma_f, l) \\ &= -\frac{1}{2}(\mathbf{y} - \mu(\mathbf{x}))^T [k(\mathbf{x}, \mathbf{x}) + C]^{-1}(\mathbf{y} - \mu(\mathbf{x})) \\ &\quad - \frac{1}{2} \ln |k(\mathbf{x}, \mathbf{x}) + C| - \frac{n}{2} \ln 2\pi, \end{aligned} \quad (2)$$

where  $C = C(\sigma(\mathbf{x}), \sigma(\mathbf{x}))$  is the covariance matrix of the data and  $n$  is the number of data. After optimizing for  $\sigma_f$  and  $l$ ,  $f(x)$  at points  $\mathbf{x}^*$  can be reconstructed as

$$\overline{f(\mathbf{x}^*)} = \mu(\mathbf{x}^*) + k(\mathbf{x}^*, \mathbf{x})[k(\mathbf{x}, \mathbf{x}) + C]^{-1}(\mathbf{y} - \mu(\mathbf{x})) \quad (3)$$

with

$$\text{cov}(f(\mathbf{x}^*)) = k(\mathbf{x}^*, \mathbf{x}^*) - k(\mathbf{x}^*, \mathbf{x})[k(\mathbf{x}, \mathbf{x}) + C]^{-1}k(\mathbf{x}, \mathbf{x}^*). \quad (4)$$

Following the above procedures, we can reconstruct the cosmic expansion history by the GP package GaPP3 [30].

### B. Pantheon+ sample

In this paper, we only use the Pantheon+ sample [9] to reconstruct  $D_L(z)$ . This dataset consists of 1701 light curves of 1550 distinct SNIa in the redshift range  $0.001 < z < 2.26$ . Here we need to transform the distribution of SNIa from the Equatorial coordinate system  $(\alpha, \delta)$  into the Galactic coordinate system  $(l, b)$ . In Fig. 1, we show the distribution of these 1550 SNIa in the Galactic coordinate system. Following the hemisphere comparison method [10, 11], we divide the full dataset into several subsets to probe the cosmic anisotropy, as listed in Tab. I. Obviously, each SNIa subset can only give the local information of the Universe.

Given the corrected apparent magnitudes  $m$  of SNIa, the information about the luminosity distance  $d_L$  of SNIa can be derived from the relation between them as

$$\begin{aligned} m &= 5 \log_{10} \left[ \frac{d_L}{1 \text{Mpc}} \right] + 25 + M \\ &= 5 \log_{10} \left[ \frac{d_L H_0 / c}{1 \text{Mpc} \cdot H_0 / c} \right] + 25 + M \\ &= 5 \log_{10} [d_L H_0 / c] - 5 \log_{10} [10 \text{pc} \cdot H_0 / c] + M, \end{aligned} \quad (5)$$

where  $M$  is the absolute magnitude of SNIa. By defining a dimensionless luminosity distance  $D_L \equiv d_L H_0 / c$  and a fiducial parameter  $M_* \equiv M - 5 \log_{10} [10 \text{pc} \cdot H_0 / c]$ , we have

$$D_L = 10^{\frac{m - M_*}{5}}. \quad (6)$$

It is worth noting that we don't know the value of  $M_*$  in fact. However we can express it as

$$\begin{aligned} M_* &= -19.3 + \delta_M - 5 \log_{10} [\delta_{70} \cdot 70 / 3^{10}] \\ &= 23.86 + \delta_M - 5 \log_{10} [\delta_{70}], \end{aligned} \quad (7)$$

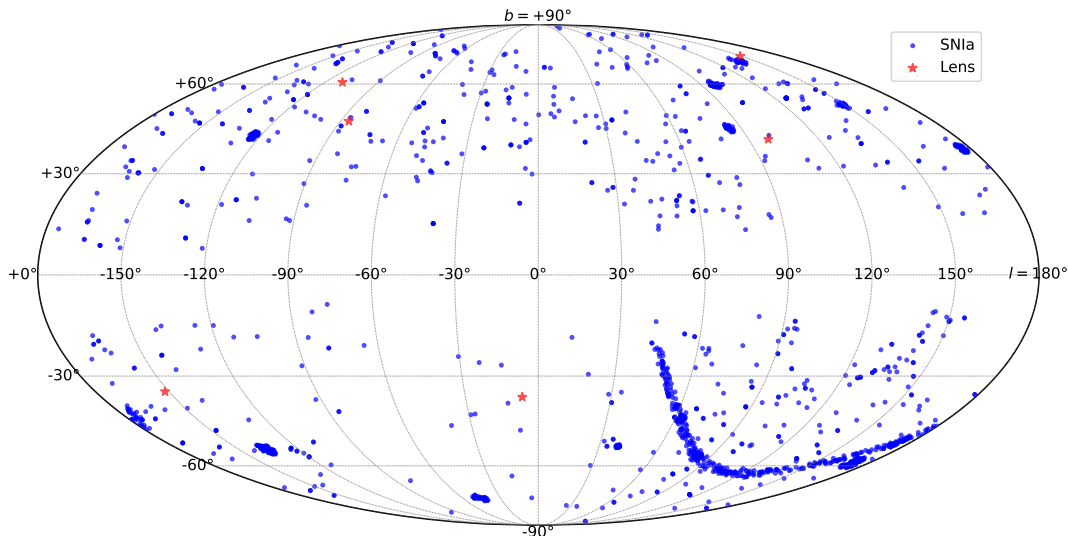


FIG. 1: The distribution of 1550 SNIa of the Pantheon+ sample [9] and 6 lenses of the H0LiCOW sample [35] in the Galactic coordinate system  $(l, b)$ , where the blue dots are SNIa and the red stars are lenses.

TABLE I: According to the distribution of 1550 SNIa of the Pantheon+ sample [9] and 6 lenses of the H0LiCOW sample [35] in the Galactic coordinate system  $(l, b)$ , the full dataset is divide into  $\text{PH}_N + \text{PH}_S$  by a division along the Galactic plane,  $\text{PH}_E + \text{PH}_W$  by a division orthogonal to the Galactic plane and  $\text{PH}_{NE} + \text{PH}_{NW} + \text{PH}_{SE} + \text{PH}_{SW}$  by both simultaneous divisions.

Dataset	$l$	$b$
$\text{PH}_{\text{All}}$	$-180^\circ \leq l < 180^\circ$	$-90^\circ \leq b \leq 90^\circ$
$\text{PH}_N$	$-180^\circ \leq l < 180^\circ$	$0^\circ \leq b \leq 90^\circ$
$\text{PH}_S$	$-180^\circ \leq l < 180^\circ$	$-90^\circ \leq b < 0^\circ$
$\text{PH}_W$	$-180^\circ \leq l < 0^\circ$	$-90^\circ \leq b \leq 90^\circ$
$\text{PH}_E$	$0^\circ \leq l < 180^\circ$	$-90^\circ \leq b \leq 90^\circ$
$\text{PH}_{NW}$	$-180^\circ \leq l < 0^\circ$	$0^\circ \leq b \leq 90^\circ$
$\text{PH}_{NE}$	$0^\circ \leq l < 180^\circ$	$0^\circ \leq b \leq 90^\circ$
$\text{PH}_{SW}$	$-180^\circ \leq l < 0^\circ$	$-90^\circ \leq b < 0^\circ$
$\text{PH}_{SE}$	$0^\circ \leq l < 180^\circ$	$-90^\circ \leq b < 0^\circ$

where  $\delta_M - 19.3 = M$  and  $\delta_{70} \cdot 70 \text{ km/s/Mpc} = H_0$  characterize the unknown information about  $M$  and  $H_0$ . Since  $M$  is the intrinsic parameter of SNIa,  $\delta M$  (or  $M$ ) should not be space-dependent or time-dependent when Newton's Constant  $G$  is supposed to be a real constant and not changing [41–43]. By isolating the anisotropic information carried by  $\delta_{70}$  (or  $H_0$ ), we can determine  $\delta_M$  from the following relation

$$\tilde{D}_L = D_L / \delta_{70} = d_L / c \cdot 70 \text{ km/s/Mpc} = 10^{\frac{m - 23.86 - \delta_M}{5}}. \quad (8)$$

If  $\delta_M$  and  $\delta_{70}$  are known, according to Eq. (6), we can obtain the covariance matrix of  $\mathbf{D}_L$  vector from the covariance matrix of  $\mathbf{m}$  vector as

$$\mathbf{C}_{D_L} = \mathbf{J} \mathbf{C}_m \mathbf{J}^T, \quad (9)$$

TABLE II: Six lenses of the H0LiCOW sample [35] in the Galactic coordinate system  $(l, b)$ , where  $z_l$  and  $z_s$  is the redshift of lens and source respectively.

Lens name	$l$	$b$	$z_l$	$z_s$
B1608 + 656	98.3397	40.8915	0.6304	1.394
RXJ1131 – 1231	-86.2504	46.8456	0.295	0.654
HE 0435 – 1223	-151.5704	-34.8188	0.4546	1.693
SDSS 1206 + 4332	148.9913	71.2445	0.745	1.789
WFI2033 – 4723	-6.6015	-36.5264	0.6575	1.662
PG 1115 + 080	-110.1126	60.6443	0.311	1.722

where  $J_{ii} = \frac{\partial D_{L,i}}{\partial m_i}$  is a diagonal Jacobian matrix. Then we can reconstruct  $D_L(z)$  with the derived data  $\{\mathbf{z}, \mathbf{D}_L, \mathbf{C}_{D_L}\}$  from the Pantheon+ sample [9]. Similarly, if only  $\delta_M$  is known, according to Eq. (8), we can reconstruct  $\tilde{D}_L(z)$  with the derived data  $\{\mathbf{z}, \tilde{\mathbf{D}}_L, \mathbf{C}_{\tilde{D}_L}\}$  from the Pantheon+ sample [9].

### C. H0LiCOW sample

The H0LiCOW sample consists of six lensed quasars [35], as listed in Tab. II. They also spread out in the Galactic coordinate system, as shown in Fig. 1. For cosmological purposes, the effective time-delay distance  $d_{\Delta t}$  of every lens system can be considered as the derived data. Because we want to use  $d_{\Delta t}$  measurements from the H0LiCOW sample [35] to anchor  $D_L(z)$  (or  $\tilde{D}_L(z)$ ) reconstructions at high redshifts. So we need to convert the dimensionless luminosity distance reconstruction  $D_L(z)$  into the dimensionless angular diameter distance reconstruction  $D_A(z) = D_L(z)/(1+z)^2$  and consequently into

the dimensionless time-delay distance of any lens system

$$D_{\Delta t} \equiv \frac{(1+z_l)D_A(z_l)(1+z_s)D_A(z_s)}{(1+z_s)D_A(z_s) - (1+z_l)D_A(z_l)} = d_{\Delta t}H_0/c, \quad (10)$$

where  $z_l$  and  $z_s$  is the redshift of lens and source respectively. To isolate the anisotropic information carried by  $H_0$ , we turn to  $\delta_{70}$  again

$$\tilde{D}_{\Delta t} = D_{\Delta t}/\delta_{70} = d_{\Delta t}/c \cdot 70 \text{ km/s/Mpc}. \quad (11)$$

### III. RESULTS

In this section, we will first determine the space-independent intrinsic parameters of SNIa,  $\delta_M$  and  $M$ . Then the space-dependent information can be determined with known  $\delta_M$  and  $M$ .

#### A. Determination of $\delta_M$ and $M$

Before testing the cosmic anisotropy, we must have a good knowledge of the space-independent parameters, such as  $\delta_M$  and  $M$ . According to Eq. (11), the likelihood is

$$\mathcal{L} = P(\tilde{\mathbf{D}}_{\Delta t}, \mathbf{d}_{\Delta t} | \delta_M, H), \quad (12)$$

where hypothesis  $H$  is that the mean value of  $c\tilde{\mathbf{D}}_{\Delta t}/\mathbf{d}_{\Delta t}$  is 70 km/s/Mpc, the data vector  $\tilde{\mathbf{D}}_{\Delta t}$  is derived from  $\tilde{D}_L(z)$  given the redshift tensor  $(z_l, z_s)$  listed in Tab. II, the corresponding data vector  $\mathbf{d}_{\Delta t}$  is given by the H0LiCOW sample [35] directly. We use the `emcee` [44] sampler to get the Monte Carlo Markov (MCMC) chain of  $\delta_M$  which has a uniform distribution prior of  $(-0.3, 0.3)$ . During the course, each sample of the MCMC chain of  $\delta_M$  is used to reconstruct  $\tilde{D}_L(z)$  from the whole Pantheon+ sample [9] according to Eq. (8) by the GP package `GaPP3` [30]. Due to the prohibitive computational cost of  $\tilde{D}_L(z)$  reconstructions with a large number of  $\delta_M$ , we have to turn to the approximation of

$$\tilde{D}_L(z, \delta_M \neq 0) \approx \tilde{D}_L(z, \delta_M = 0) 10^{-\frac{\delta_M}{5}}. \quad (13)$$

That is to say, we just reconstruct  $\tilde{D}_L(z, \delta_M = 0)$  once. Then we obtain  $\tilde{D}_L(z, \delta_M \neq 0)$  reconstructions by adjusting the reconstruction of  $\tilde{D}_L(z, \delta_M = 0)$  with  $10^{-\frac{\delta_M}{5}}$ , including the mean value and the uncertainty. Finally, we get the posterior probability density function (PDF) of  $\delta_M = 0.0478_{-0.0279}^{+0.0270}$  (at 68% CL), as shown in the left panel of Fig. 2. Also we show the reconstruction of  $\tilde{D}_L(z, \delta_M = 0.0478)$  in the right panel of Fig. 2. We can find that  $\delta_M > 0$  suppresses  $\tilde{D}_L(z)$  and narrows its uncertainty, which agrees with the above approximation, Eq. (13).

#### B. Reconstruction of $d_L(z)$

Given  $M = -19.2522_{-0.0279}^{+0.0270}$  (at 68% CL), we can reconstruct  $d_L(z)$  according to Eq. (5). To probe the cosmic anisotropy, we compare the reconstruction of  $d_L(z)$  from every dataset listed in Tab. I, such as PH<sub>N</sub> vs. PH<sub>S</sub> as shown in the left panel of Fig. 3, PH<sub>W</sub> vs. PH<sub>E</sub> as shown in the left panel of Fig. 4 or PH<sub>NW</sub> vs. PH<sub>NE</sub> vs. PH<sub>SW</sub> vs. PH<sub>SE</sub> as shown in the left panel of Fig. 5. We can find that  $d_L(z)$  reconstructions from PH<sub>N</sub> and PH<sub>S</sub> are consistent with each other, as shown in the left panel of Fig. 3. Similarly,  $d_L(z)$  reconstructions from PH<sub>W</sub> and PH<sub>E</sub> are also consistent with each other, as shown in the left panel of Fig. 4. However,  $d_L(z)$  reconstructions from PH<sub>NW</sub> and PH<sub>SW</sub> are not very consistent with each other at higher redshift at 68% CL, as shown in the left panel of Fig. 5. This over  $1\sigma$  inconsistency can be regarded as a weak preference for the cosmic anisotropy. Since we reconstruct  $d_L(z)$  directly, the anisotropic information maybe carried by the Hubble parameter  $H(z)$  or the cosmic curvature  $\Omega_k$  has been included as  $d_L(z) = d_L(z, H(z), \Omega_k)$  even though there is no specific cosmological model to be assumed. Therefore, we can not tell the source of this cosmic anisotropy is the dark energy or the cosmic curvature.

In fact, the above inconsistency between  $d_L(z)$  reconstructions can also result from the inconsistency between data or the paucity of data. Therefore, we use the prediction of  $d_{\Delta t}$  from different dataset to do the consistency test. Firstly, we define

$$I \equiv \frac{1}{N} \sum_{i=1}^N \frac{d_{\Delta t,i}^P}{d_{\Delta t,i}^H}, \quad (14)$$

where  $d_{\Delta t,i}^H$  is the measured effective time-delay distance of  $i$ -th lens system of a certain dataset listed in Tab. I and  $d_{\Delta t,i}^P$  is the derived one from the partial Pantheon+ sample from the same dataset. We compare the constraints on  $I$  from every dataset listed in Tab. I, such as PH<sub>N</sub> vs. PH<sub>S</sub> as shown in the right panel of Fig. 3, PH<sub>W</sub> vs. PH<sub>E</sub> as shown in the right panel of Fig. 4 or PH<sub>NW</sub> vs. PH<sub>NE</sub> vs. PH<sub>SW</sub> as shown in the right panel of Fig. 5. We can find that  $I = 1.0289_{-0.0732}^{+0.0793}$  (at 68% CL) from PH<sub>N</sub> is consistent with  $I = 0.9587_{-0.0576}^{+0.0577}$  (at 68% CL) from PH<sub>S</sub>;  $I = 1.0045_{-0.0689}^{+0.0702}$  (at 68% CL) from PH<sub>W</sub> is consistent with  $I = 0.9908_{-0.0683}^{+0.0842}$  (at 68% CL) from PH<sub>E</sub>;  $I = 1.1071_{-0.0814}^{+0.1541}$  (at 68% CL) from PH<sub>NW</sub>,  $I = 0.9984_{-0.0891}^{+0.1075}$  (at 68% CL) from PH<sub>NE</sub> and  $I = 0.9288_{-0.0795}^{+0.0801}$  (at 68% CL) from PH<sub>SW</sub> are almost consistent with each other; all of them are almost consistent with  $I = 1$ . (Since there is no  $d_{\Delta t,i}^H$  in PH<sub>SE</sub> dataset, there is no constraint on  $I$  from this dataset.) That is to say, the data we used is almost self-consistent and the over  $1\sigma$  inconsistency between  $d_L(z)$  reconstructions from PH<sub>NW</sub> and PH<sub>SW</sub> should result from the cosmic anisotropy. However, the preference for the cosmic anisotropy is so weak that we should confirm it further

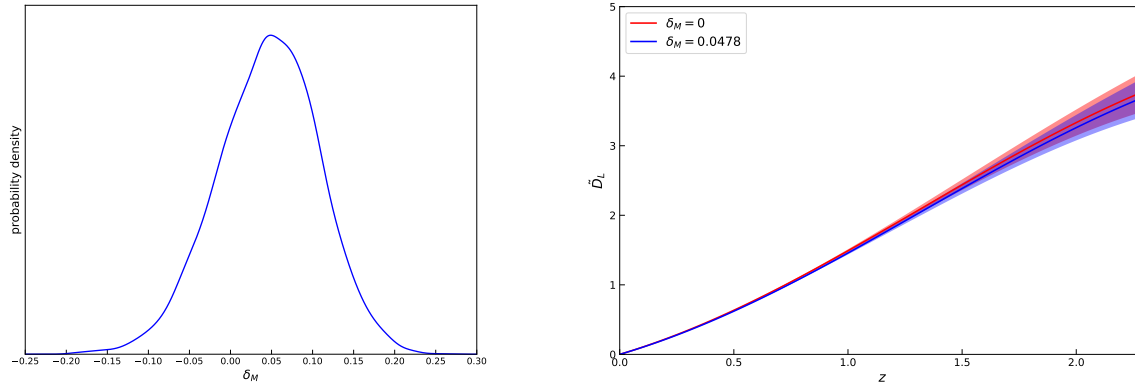


FIG. 2: LEFT: The posterior PDF of  $\delta_M$ . RIGHT: Reconstruction of  $\tilde{D}_L(z, \delta_M = 0)$  (red curve) and  $\tilde{D}_L(z, \delta_M = 0.0478)$  (blue curve) from the whole Pantheon+ sample [9] according to Eq. (8) by the GP package GaPP3 [30], where the shaded regions are the 68% CL of the reconstructions.

by other methods.

#### IV. SUMMARY AND DISCUSSION

In this paper, we try to use  $d_L(z)$  reconstruction from different dataset to probe the cosmic anisotropy. At the beginning, however, we have no knowledge of  $M$  which is also degenerate with  $H_0$ . Therefore, we turn to Eq. (8) to isolate the unknown information of  $H_0$  and then do the reconstruction of  $\tilde{D}_L(z)$  from the whole Pantheon+ sample [9] according to this equation with a parameter  $\delta_M$ . By anchoring  $\tilde{D}_L(z)$  reconstruction with the whole H0LiCOW sample [35], the information of  $M$  can be obtained,  $M = -19.2522^{+0.0270}_{-0.0279}$  (at 68% CL). Finally, we incorporate the unknown information of  $H_0$  and  $\Omega_k$  into  $d_L(z)$  and do the reconstruction of  $d_L(z)$  from different dataset listed in Tab. I according to Eq. (5). We find that  $d_L(z)$  reconstructions from these datasets making up the complete Pantheon+ sample are almost consistent with each other, as shown in the left panel of Fig. 3, Fig. 4 and Fig. 5, except that  $d_L(z)$  reconstructions from PH<sub>NW</sub> and

PH<sub>SW</sub> are not very consistent with each other at higher redshift at 68% CL, as shown in the left panel of Fig. 5. After a consistency test, we find a very weak preference for the cosmic anisotropy.

The method applied in our paper can not constrain some important cosmological parameters, such  $H_0$  or  $\Omega_k$ . Even though they can carry the anisotropic information and the constraints on  $H_0$  can help deal with the Hubble tension, the direct reconstruction of  $d_L(z)$  has given up these advantages. Of course, the direct reconstruction of  $H(z)$  is a good idea which can further give constraints on  $H_0$  or  $\Omega_k$  as did in [36]. However, our method has given up the fiducial relation  $M_* = -19.3 - 5 \log_{10}[70/3^{10}]$  and the presence of two new parameters  $\delta_M$  and  $\delta_{70}$  makes the direct reconstruction of  $H(z)$  impossible.

#### Acknowledgments

Ke Wang is supported by grants from NSFC (grant No.12247101).

- 
- [1] N. Aghanim *et al.* [Planck], “Planck 2018 results. VI. Cosmological parameters,” *Astron. Astrophys.* **641**, A6 (2020) [erratum: *Astron. Astrophys.* **652**, C4 (2021)] [arXiv:1807.06209 [astro-ph.CO]].
- [2] T. M. C. Abbott *et al.* [DES], “Dark Energy Survey Year 3 results: Cosmological constraints from galaxy clustering and weak lensing,” *Phys. Rev. D* **105**, no.2, 023520 (2022) [arXiv:2105.13549 [astro-ph.CO]].
- [3] T. M. C. Abbott *et al.* [DES], “Dark Energy Survey: A 2.1% Measurement of the Angular Baryonic Acoustic Oscillation Scale at Redshift  $z_{\text{eff}}=0.85$  from the Final Dataset,” [arXiv:2402.10696 [astro-ph.CO]].
- [4] S. Alam *et al.* [eBOSS], “Completed SDSS-IV extended Baryon Oscillation Spectroscopic Survey: Cosmological implications from two decades of spectroscopic surveys at the Apache Point Observatory,” *Phys. Rev. D* **103**, no.8, 083533 (2021) [arXiv:2007.08991 [astro-ph.CO]].
- [5] A. G. Adame *et al.* [DESI], “DESI 2024 VI: Cosmological Constraints from the Measurements of Baryon Acoustic Oscillations,” [arXiv:2404.03002 [astro-ph.CO]].
- [6] N. J. Secrest, S. von Hausegger, M. Rameez, R. Mohayaee, S. Sarkar and J. Colin, “A Test of the Cosmo-

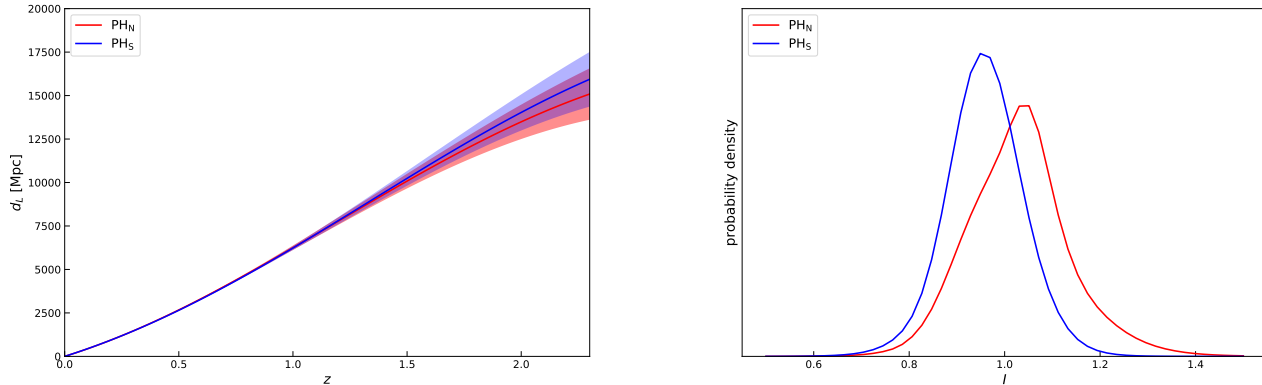


FIG. 3: LEFT: Reconstruction of  $d_L(z, \delta_M = 0.0478)$  from PH<sub>N</sub> dataset (red) and PH<sub>S</sub> dataset (blue), where the shaded regions are the 68% CL of the reconstructions. RIGHT: Constraints on  $I$  from PH<sub>N</sub> dataset (red) and PH<sub>S</sub> dataset (blue).

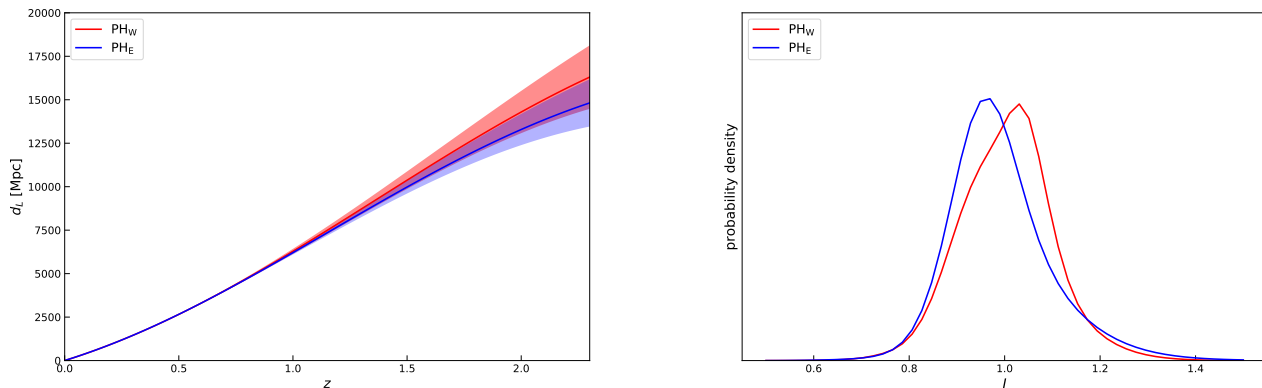


FIG. 4: LEFT: Reconstruction of  $d_L(z, \delta_M = 0.0478)$  from PH<sub>W</sub> dataset (red) and PH<sub>E</sub> dataset (blue), where the shaded regions are the 68% CL of the reconstructions. RIGHT: Constraints on  $I$  from PH<sub>W</sub> dataset (red) and PH<sub>E</sub> dataset (blue).

logical Principle with Quasars,” *Astrophys. J. Lett.* **908**, no.2, L51 (2021) [arXiv:2009.14826 [astro-ph.CO]].

- [7] P. A. R. Ade *et al.* [Planck], “Planck 2015 results. XXIV. Cosmology from Sunyaev-Zeldovich cluster counts,” *Astron. Astrophys.* **594**, A24 (2016) [arXiv:1502.01597 [astro-ph.CO]].
- [8] A. G. Riess, W. Yuan, L. M. Macri, D. Scolnic, D. Brout, S. Casertano, D. O. Jones, Y. Murakami, L. Breuval and T. G. Brink, *et al.* “A Comprehensive Measurement of the Local Value of the Hubble Constant with 1 km s<sup>-1</sup> Mpc<sup>-1</sup> Uncertainty from the Hubble Space Telescope and the SH0ES Team,” *Astrophys. J. Lett.* **934**, no.1, L7 (2022) [arXiv:2112.04510 [astro-ph.CO]].
- [9] D. Brout, D. Scolnic, B. Popovic, A. G. Riess, J. Zuntz, R. Kessler, A. Carr, T. M. Davis, S. Hinton and

D. Jones, *et al.* “The Pantheon+ Analysis: Cosmological Constraints,” *Astrophys. J.* **938**, no.2, 110 (2022) [arXiv:2202.04077 [astro-ph.CO]].

- [10] D. J. Schwarz and B. Weinhorst, “(An)isotropy of the Hubble diagram: Comparing hemispheres,” *Astron. Astrophys.* **474**, 717-729 (2007) [arXiv:0706.0165 [astro-ph]].
- [11] I. Antoniou and L. Perivolaropoulos, “Searching for a Cosmological Preferred Axis: Union2 Data Analysis and Comparison with Other Probes,” *JCAP* **12**, 012 (2010) [arXiv:1007.4347 [astro-ph.CO]].
- [12] K. M. Górski, E. Hivon, A. J. Banday, B. D. Wandelt, F. K. Hansen, M. Reinecke and M. Bartelman, “HEALPix - A Framework for high resolution discretization, and fast analysis of data distributed on the

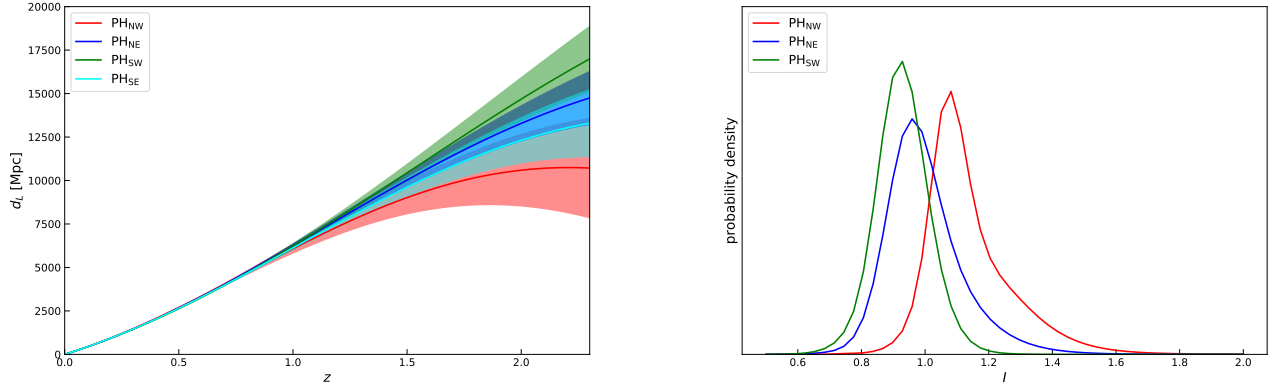


FIG. 5: LEFT: Reconstruction of  $d_L(z, \delta_M = 0.0478)$  from PH<sub>NW</sub> dataset (red), PH<sub>NE</sub> dataset (blue), PH<sub>SW</sub> dataset (green) and PH<sub>SE</sub> dataset (cyan), where the shaded regions are the 68% CL of the reconstructions. RIGHT: Constraints on  $I$  from PH<sub>NW</sub> dataset (red), PH<sub>NE</sub> dataset (blue) and PH<sub>SW</sub> dataset (green). Since there is no  $H_{\Delta t, i}^H$  in PH<sub>SE</sub> dataset, there is no constraint on  $I$  from this dataset.

- sphere,” *Astrophys. J.* **622**, 759-771 (2005) [arXiv:astro-ph/0409513 [astro-ph]].
- [13] A. Mariano and L. Perivolaropoulos, “Is there correlation between Fine Structure and Dark Energy Cosmic Dipoles?,” *Phys. Rev. D* **86**, 083517 (2012) [arXiv:1206.4055 [astro-ph.CO]].
- [14] H. K. Deng and H. Wei, “Testing the Cosmic Anisotropy with Supernovae Data: Hemisphere Comparison and Dipole Fitting,” *Phys. Rev. D* **97**, no.12, 123515 (2018) doi:10.1103/PhysRevD.97.123515 [arXiv:1804.03087 [astro-ph.CO]].
- [15] Z. Q. Sun and F. Y. Wang, “Testing the anisotropy of cosmic acceleration from Pantheon supernovae sample,” *Mon. Not. Roy. Astron. Soc.* **478**, no.4, 5153-5158 (2018) [arXiv:1805.09195 [astro-ph.CO]].
- [16] H. K. Deng and H. Wei, “Null signal for the cosmic anisotropy in the Pantheon supernovae data,” *Eur. Phys. J. C* **78**, no.9, 755 (2018) [arXiv:1806.02773 [astro-ph.CO]].
- [17] D. Zhao, Y. Zhou and Z. Chang, “Anisotropy of the Universe via the Pantheon supernovae sample revisited,” *Mon. Not. Roy. Astron. Soc.* **486**, no.4, 5679-5689 (2019) [arXiv:1903.12401 [astro-ph.CO]].
- [18] J. P. Hu, Y. Y. Wang, J. Hu and F. Y. Wang, “Testing the cosmological principle with the Pantheon+ sample and the region-fitting method,” *Astron. Astrophys.* **681**, A88 (2024) [arXiv:2310.11727 [astro-ph.CO]].
- [19] W. Zhao, P. X. Wu and Y. Zhang, “Anisotropy of Cosmic Acceleration,” *Int. J. Mod. Phys. D* **22**, 1350060 (2013) [arXiv:1305.2701 [astro-ph.CO]].
- [20] H. N. Lin, S. Wang, Z. Chang and X. Li, “Testing the isotropy of the Universe by using the JLA compilation of type-Ia supernovae,” *Mon. Not. Roy. Astron. Soc.* **456**, no.2, 1881-1885 (2016) [arXiv:1504.03428 [astro-ph.CO]].
- [21] Z. Chang, D. Zhao and Y. Zhou, “Constraining the anisotropy of the Universe with the Pantheon supernovae sample,” *Chin. Phys. C* **43**, no.12, 125102 (2019) [arXiv:1910.06883 [astro-ph.CO]].
- [22] K. Wang, K. P. Chen and M. Le Delliou, “Constraints on the local cosmic void from the Pantheon supernovae data,” *Eur. Phys. J. C* **83**, no.9, 859 (2023) [arXiv:2304.13945 [astro-ph.CO]].
- [23] İ. Semiz and A. K. Çamlıbel, “What do the cosmological supernova data really tell us?,” *JCAP* **12**, 038 (2015) [arXiv:1505.04043 [gr-qc]].
- [24] A. K. Çamlıbel, İ. Semiz and M. A. Feyizoğlu, “Pantheon update on a model-independent analysis of cosmological supernova data,” *Class. Quant. Grav.* **37**, no.23, 235001 (2020) doi:10.1088/1361-6382/abba48 [arXiv:2001.04408 [astro-ph.CO]].
- [25] T. Collett, F. Montanari and S. Rasanen, “Model-Independent Determination of  $H_0$  and  $\Omega_{K0}$  from Strong Lensing and Type Ia Supernovae,” *Phys. Rev. Lett.* **123**, no.23, 231101 (2019) [arXiv:1905.09781 [astro-ph.CO]].
- [26] U. Andrade, C. A. P. Bengaly, B. Santos and J. S. Alcaniz, “A Model-independent Test of Cosmic Isotropy with Low- $z$  Pantheon Supernovae,” *Astrophys. J.* **865**, no.2, 119 (2018) [arXiv:1806.06990 [astro-ph.CO]].
- [27] C. Cattoen and M. Visser, “Cosmography: Extracting the Hubble series from the supernova data,” [arXiv:gr-qc/0703122 [gr-qc]].
- [28] G. J. Wang, X. J. Ma, S. Y. Li and J. Q. Xia, “Reconstructing Functions and Estimating Parameters with Artificial Neural Networks: A Test with a Hubble Parameter and SNe Ia,” *Astrophys. J. Suppl.* **246**, no.1, 13 (2020) [arXiv:1910.03636 [astro-ph.CO]].
- [29] J. F. Jesus, R. Valentim, A. A. Escobal and S. H. Pereira, “Gaussian Process Estimation of Transition Redshift,” *JCAP* **04**, 053 (2020) [arXiv:1909.00090 [astro-ph.CO]].
- [30] M. Seikel, C. Clarkson and M. Smith, “Reconstruction of dark energy and expansion dynamics using Gaussian processes,” *JCAP* **06**, 036 (2012) [arXiv:1204.2832 [astro-ph.CO]].
- [31] É. Aubourg *et al.* [BOSS], “Cosmological implications of baryon acoustic oscillation measurements,” *Phys. Rev. D* **92**, no.12, 123516 (2015) [arXiv:1411.1074 [astro-

- ph.CO]].
- [32] A. J. Cuesta, L. Verde, A. Riess and R. Jimenez, “Calibrating the cosmic distance scale ladder: the role of the sound horizon scale and the local expansion rate as distance anchors,” *Mon. Not. Roy. Astron. Soc.* **448**, no.4, 3463-3471 (2015) [arXiv:1411.1094 [astro-ph.CO]].
- [33] P. L. Kelly, S. Rodney, T. Treu, M. Oguri, W. Chen, A. Zitrin, S. Birrer, V. Bonvin, L. Dessart and J. M. Diego, *et al.* “Constraints on the Hubble constant from supernova Refsdal’s reappearance,” *Science* **380**, no.6649, abh1322 (2023) [arXiv:2305.06367 [astro-ph.CO]].
- [34] X. Li and K. Liao, “Determining Cosmological-model-independent  $H_0$  with Gravitationally Lensed Supernova Refsdal,” *Astrophys. J.* **966**, no.1, 121 (2024) [arXiv:2401.12052 [astro-ph.CO]].
- [35] K. C. Wong, S. H. Suyu, G. C. F. Chen, C. E. Rusu, M. Millon, D. Sluse, V. Bonvin, C. D. Fassnacht, S. Taubenberger and M. W. Auger, *et al.* “H0LiCOW – XIII. A 2.4 per cent measurement of  $H_0$  from lensed quasars:  $5.3\sigma$  tension between early- and late-Universe probes,” *Mon. Not. Roy. Astron. Soc.* **498**, no.1, 1420-1439 (2020) [arXiv:1907.04869 [astro-ph.CO]].
- [36] K. Liao, A. Shafieloo, R. E. Keeley and E. V. Linder, “A model-independent determination of the Hubble constant from lensed quasars and supernovae using Gaussian process regression,” *Astrophys. J. Lett.* **886**, no.1, L23 (2019) [arXiv:1908.04967 [astro-ph.CO]].
- [37] S. Taubenberger, S. H. Suyu, E. Komatsu, I. Jee, S. Birrer, V. Bonvin, F. Courbin, C. E. Rusu, A. J. Shajib and K. C. Wong, “The Hubble Constant determined through an inverse distance ladder including quasar time delays and Type Ia supernovae,” *Astron. Astrophys.* **628**, L7 (2019) [arXiv:1905.12496 [astro-ph.CO]].
- [38] K. Liao, A. Shafieloo, R. E. Keeley and E. V. Linder, “Determining Model-independent  $H_0$  and Consistency Tests,” *Astrophys. J. Lett.* **895**, no.2, L29 (2020) [arXiv:2002.10605 [astro-ph.CO]].
- [39] X. Li, R. E. Keeley, A. Shafieloo and K. Liao, “A Model-independent Method to Determine  $H_0$  Using Time-delay Lensing, Quasars, and Type Ia Supernovae,” *Astrophys. J.* **960**, no.2, 103 (2024) [arXiv:2308.06951 [astro-ph.CO]].
- [40] A. Shafieloo, A. G. Kim and E. V. Linder, “Gaussian Process Cosmography,” *Phys. Rev. D* **85**, 123530 (2012) [arXiv:1204.2272 [astro-ph.CO]].
- [41] W. Zhao, B. S. Wright and B. Li, “Constraining the time variation of Newton’s constant  $G$  with gravitational-wave standard sirens and supernovae,” *JCAP* **10**, 052 (2018) [arXiv:1804.03066 [astro-ph.CO]].
- [42] K. Wang and L. Chen, “Constraints on Newton’s constant from cosmological observations,” *Eur. Phys. J. C* **80**, no.6, 570 (2020) [arXiv:2004.13976 [astro-ph.CO]].
- [43] Y. Liu, H. Yu and P. Wu, “Alleviating the Hubble-constant tension and the growth tension via a transition of absolute magnitude favored by the Pantheon+ sample,” *Phys. Rev. D* **110**, no.2, L021304 (2024) [arXiv:2406.02956 [astro-ph.CO]].
- [44] D. Foreman-Mackey, D. W. Hogg, D. Lang and J. Goodman, “emcee: The MCMC Hammer,” *Publ. Astron. Soc. Pac.* **125**, 306-312 (2013) [arXiv:1202.3665 [astro-ph.IM]].